Title: Impact of the Heat and Thermal radiation on Phan Thien Tanner Fluid Model Obeying Peristaltic Mechanism with Permeable Wall

Manuscript ID: IJST-2024-2261

Type: Research Article

Keywords: PTT fluid, Peristaltic flow, Heat transfer, Thermal Radiation, Permeable wall

Journal: Indian Journal of Science and Technology

Authors

1. Mahadev Channakote (Corresponding author)

Abstract

Objectives: The primary objective of the current exploration is to discuss the novel aspects of the peristaltic flow of a Phan-Thien-Tanner (PTT) fluid in a planar channel. This study aims to understand the behavior and characteristics of this specific type of fluid flow under peristaltic pumping. The PTT fluid is a viscoelastic fluid model that accounts for both the viscous and elastic properties of the fluid. Additionally, the effects of heat and thermal radiation are considered to provide a comprehensive understanding of the flow dynamics. Methods: The mathematical model is formulated using the continuity equation, momentum equation, and energy equation. The continuity equation provides insights into the fluid flow and behavior within the channel. The momentum equation describes the fluid's motion and governs the resultant force exerted on the flow boundaries. The energy equation explains the conversion of mechanical energy into thermal energy. To account for the non-Newtonian nature of the fluid, the Phan-Thien-Tanner constitutive equation is employed. We utilize long-wavelength and low-Reynolds number approximations to simplify the channel's flow characteristics Findings: The study derives expressions for velocity, pressure, pressure gradient, and heat transfer. The effects of various physical parameters, including the Brinkman number (Br) and the Weissenberg number (We), on pumping phenomena, velocity, temperature, pressure, and pressure gradient are analyzed through graphical representations. The results are discussed in detail, highlighting the influence of these parameters on the flow dynamics Novelty: The novelty of this work lies in the simultaneous consideration of heat transfer, thermal radiation, peristaltic flow, permeable wall conditions, and the behaviors of Pan-Thien Tanner and viscoelastic fluids. This approach is expected to significantly impact the development and enhancement of various drug delivery systems in the biomedical industry.

Impact of the Heat and Thermal radiation on Phan Thien Tanner Fluid Model Obeying Peristaltic Mechanism with Permeable Wall

Mahadev M Channakote

Department of Mathematics and Statistics, M.S. Ramaiah University of Applied Sciences, Bengaluru, Karnataka, India

Corresponding Author: mchannakote@rediffmail.com

Mahalakshmi B. R

Department of Mathematics and Statistics, M.S. Ramaiah University of Applied Sciences, Bengaluru, Karnataka, India

Email ID: mahalakshmibr02@gmail.com

Shivakumar Biradar

Department of Mathematics, Government First Grade College, Chitaguppa, Karnataka, India

Email ID: shivubrdr@gmail.com

Impact of the Heat and Thermal radiation on Phan Thien Tanner Fluid Model Obeying Peristaltic Mechanism with Permeable Wall

Abstract:

Objectives: The primary objective of the current exploration is to discuss the novel aspects of the peristaltic flow of a Phan-Thien-Tanner (PTT) fluid in a planar channel. This study aims to understand the behavior and characteristics of this specific type of fluid flow under peristaltic pumping. The PTT fluid is a viscoelastic fluid model that accounts for both the viscous and elastic properties of the fluid. Additionally, the effects of heat and thermal radiation are considered to provide a comprehensive understanding of the flow dynamics.

Methods: The mathematical model is formulated using the continuity equation, momentum equation, and energy equation. The continuity equation provides insights into the fluid flow and behavior within the channel. The momentum equation describes the fluid's motion and governs the resultant force exerted on the flow boundaries. The energy equation explains the conversion of mechanical energy into thermal energy. To account for the non-Newtonian nature of the fluid, the Phan-Thien-Tanner constitutive equation is employed. We utilize long-wavelength and low-Reynolds number approximations to simplify the channel's flow characteristics

Findings: The study derives expressions for velocity, pressure, pressure gradient, and heat transfer. The effects of various physical parameters, including the Brinkman number (Br) and the Weissenberg number (We), on pumping phenomena, velocity, temperature, pressure, and pressure gradient are analyzed through graphical representations. The results are discussed in detail, highlighting the influence of these parameters on the flow dynamics

Novelty: The novelty of this work lies in the simultaneous consideration of heat transfer, thermal radiation, peristaltic flow, permeable wall conditions, and the behaviors of Pan-Thien Tanner and viscoelastic fluids. This approach is expected to significantly impact the development and enhancement of various drug delivery systems in the biomedical industry.

Keywords: PTT fluid, Peristaltic flow, Heat transfer, Thermal Radiation, Permeable wall

1. Introduction

Peristalsis, a wave-like pattern of muscle contraction, is responsible for pumping physiological fluids from one location to another through muscular contractions. These contractions originate in our digestive system and are a natural and inevitable part of its function. The ureter, which connects the kidney and bladder, also exhibits peristaltic movement. Due to its crucial role, peristaltic flow is widely utilized for both physiological and mechanical purposes under various conditions. Additionally, its applications extend to numerous industries, including nuclear, ceramic, porcelain, oil, industrial, paper, and food sectors, where it is employed on a daily basis. The concept of fluid movement through peristaltic transfer was first introduced by Latham [1] and Shapiro et al. [2]. Since then, numerous researchers have worked to develop peristaltic transport influenced by different physical properties across various media, yielding promising results. Later on, a very substantial study has been reported by the theoretical and experimental approach. Researchers have done great work in this era. [3-11].

Recent breakthroughs have enabled significant practical applications for investigating peristaltic transport using PTT liquid in various geometrical forms across several sectors and physiological domains. This mechanism is utilized in the medical and physiological fields to develop artificial heart-lung machines and to ensure the safe evacuation of hazardous liquids from nuclear power plants, among other applications. The PTT constitutive equation makes accurate predictions about the rheology of various concentrated polymer solutions and melts (Phan-Thien and Tanner). In procedures involving high temperature and heat transfer operations, these fluid models are widely employed to resemble real fluids. It is now well acknowledged that the majority of biofluids in nature behave as non-Newtonian fluids. Hakeem and Naby [12] use a Phan-Thien-Tanner (PTT) fluid model to simulate the complicated dynamics of chyme in the small intestine, and they find good agreement between their theoretical and experimental findings. And many other researchers like Vajravelu et al. [13], Hayat et al. [14], Abd El Hakeem and Abd El Naby [15], Siddiqui et al.[16], Hayat, et al. [17], Mahadev and Axita[18], Vajravelu et al.[19]. Channakote et al.[20].

Due to its various applications in petroleum reservoir rocks, slurries, sedimentation, and sand beds the flow through porous medium received considerable attention by researchers and scientists. Examples of porous medium in the human body include small blood vessels, human lungs, stone gall bladder, bile ducts etc. Applying generalized Darcy’s law peristaltic flow through a porous medium has been investigated by several researchers. Researcher’s like Vajravelu et al. [21] have discussed about the peristaltic transport in channel through porous medium by permeable wall. Radhakrishnamacharya and Radhakrishnamurty [22] studied the peristaltic flow and heat transfer in a vertical porous medium. Channakote and Kalse [23] studied about the heat transfer in peristaltic motion of Rabinowitsch fluid in a channel with permeable wall. Some relevant studies on the topic can be found from the list of references [24-28].

The study of bioheat transfer and thermal radiation in tissues has attracted many investigators due to its applications in thermotherapy and human thermoregulation systems. Additionally, understanding heat transfer in relation to peristalsis is crucial because it plays a significant role in physiology. For example, the thermodynamic properties of blood are vital for oxygenation and hemodialysis. Thermal radiation is now effectively utilized in many high-temperature processes. Various industrial companies have made numerous submissions regarding strategies for nuclear power plants. Sunitha and Asha [29] discussed the effect of heat radiation on the peristaltic blood motion of a Jeffrey liquid involving double diffusion with gold nanoparticles. Kothandapani et al. [30] conferred the consequences of heat radiation on peristaltic transportation. In a non-uniform inclined tube, Rafiq and Abbas [31] examined the outcomes of thermal radiation and viscous dissipation on the peristaltic flow of the Rabinowitsch viscoelastic fluid. Hayat et al. [32] elucidated the magneto Nanofluid flow in a porous channel with the radiative peristaltic flow and thermal radiation. Impact of electro-osmosis and Joule heating effects on peristaltic transport with thermal radiation of hyperbolic tangent fluid through a porous media in an endoscope has been discussed by Asha and Vijayalaxmi [33]. Channakote and Siddabasappa[34] explored the study of heat and mass transfer on peristaltic flow of Pan-Thien

Tanner li1uid with wall properties. Channakote *et al.* [35] considered Ellis rheological fluid peristaltic pumping in a non-uniform tube with viscous dissipation and convective heat transfer. This approach for examining peristaltic transport under varied flow configurations with varying geometries has been provided in recent research. [35]–[40]).

The aforementioned impacts have motivated us to investigate the influence of thermal radiation on the Phan-Thien-Tanner (PTT) fluid model within a peristaltic mechanism with permeable walls. The PTT fluid is significant for its shear thickening, shear thinning, and time relaxation properties. Our primary focus will be on analyzing the effects of various parameters on velocity, pressure, and temperature. The mathematical modeling is conducted using long wavelength and low Reynolds number approximations. The resulting equations are numerically solved using Mathematica software. The effects of various parameters on velocity, temperature, pressure rise, and the trapping phenomenon are discussed through graphical representations.

Physical model

The extra stress tensor for linear Phan-Thien and Tanner (PTT) fluid model is [Vajravelu (19) Hayat (19)]

$$T = -pI + \tau ,$$
(1)

$f¿$ (2)

$$\tau^{\nabla} = \frac{d\tau}{dt} - \tau . L' - L . \tau ,$$
(3)

$$f\left(tr\left(\tau\right)\right) = 1 + \frac{\epsilon\kappa}{\mu} tr\left(\tau\right) ,$$
(4)

Where, $L = grad\, V .$, p is the pressure, I is the identity tensor, μ is the dynamic viscosity, τ is the extra stress tensor, D is the deformation rate tensor, K is the relaxation time , τ^{∇} is the Oldroyds's upper convicted derivative, $\frac{d}{dt}$ is the material derivative, tr is the trace prime is the transpose.

Mathematical Formulation:

The geometric model of bio-heat transfer and thermal radiation in the peristaltic flow of an incompressible viscoelastic fluid is illustrated in Figure 1. This study examines the peristaltic flow dynamics of an incompressible Phan-Thien and Tanner (PTT) fluid model within a planar channel. The region above the permeable wall represents porous media, while the region below represents fluid flow. The motion is induced by infinite wave trains with a constant speed c, wavelength λ, and amplitude b, using a fixed rectangular coordinate frame.

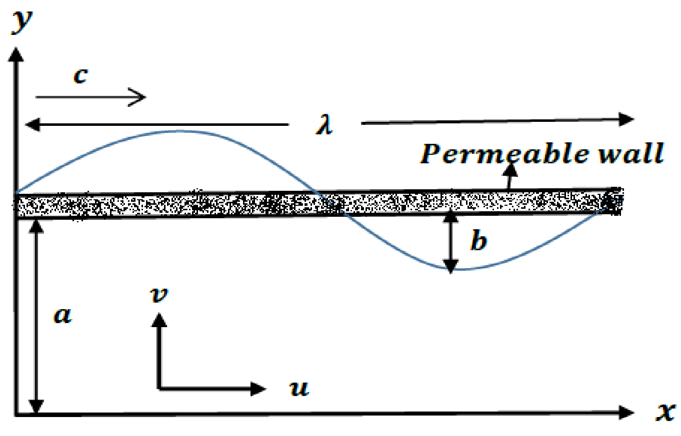

Figure.1 Flow geometry of the problem

The geometry of deforming channel walls is simulated with:

$$h(\acute{x},\acute{t})=a+b\sin\left(\frac{2\pi}{\lambda}(\acute{X}-c\acute{t})\right),$$

(5)

in which a is half width of the channel, b is wave amplitude, λ is wavelength, c is wave speed, $\acute{t}$ is time.

The equations, which can govern the present flow circumstances, are:

Continuity equation:

$$\frac{\partial \acute{u}}{\partial x}+\frac{\partial \acute{v}}{\partial y}=0,$$

(6)

Momentum equation

$$\rho\left(\acute{u}\frac{\partial \acute{u}}{\partial \acute{x}}+\acute{v}\frac{\partial \acute{u}}{\partial \acute{y}}\right)=\frac{-\partial \acute{p}}{\partial \acute{x}}+\frac{\partial \acute{\tau}_{xx}}{\partial \acute{x}}+\frac{\partial \acute{\tau}_{xy}}{\partial \acute{y}}$$

(7)

$$\rho\left(\acute{u}\frac{\partial \acute{v}}{\partial \acute{x}}+\acute{v}\frac{\partial \acute{v}}{\partial \acute{y}}\right)=\frac{-\partial \acute{p}}{\partial \acute{y}}+\frac{\partial \acute{\tau}_{yx}}{\partial \acute{x}}+\frac{\partial \acute{\tau}_{yy}}{\partial \acute{y}}$$

(8)

Energy equation:

$$\rho c_p\left(\acute{u}\frac{\partial \acute{T}}{\partial \acute{x}}+\acute{v}\frac{\partial \acute{T}}{\partial \acute{y}}\right)=K\left(\frac{\partial^2 \acute{T}}{\partial \acute{x}^2}+\frac{\partial^2 \acute{T}}{\partial \acute{y}^2}\right)+\acute{\tau}_{xx}\frac{\partial \acute{u}}{\partial \acute{x}}+\acute{\tau}_{yy}\frac{\partial \acute{v}}{\partial \acute{y}}+\acute{\tau}_{xy}\left(\frac{\partial \acute{u}}{\partial \acute{y}}+\frac{\partial \acute{v}}{\partial \acute{x}}\right)+\frac{\partial}{\partial \acute{y}}(\acute{q}_r)$$

(9)

Fluid equation:

$$f\acute{\tau}_{xx}+k\left(\acute{u}\frac{\partial\acute{\tau}_{xx}}{\partial\acute{x}}+\acute{v}\frac{\partial\acute{\tau}_{xx}}{\partial\acute{y}}-2\frac{\partial\acute{u}}{\partial\acute{x}}\acute{\tau}_{xx}-2\frac{\partial\acute{u}}{\partial\acute{y}}\acute{\tau}_{xy}\right)=2\mu\frac{\partial\acute{u}}{\partial\acute{x}} \quad (10)$$

$$f\acute{\tau}_{yy}+k\left(\acute{u}\frac{\partial\acute{\tau}_{yy}}{\partial\acute{x}}+\acute{v}\frac{\partial\acute{\tau}_{yy}}{\partial\acute{y}}-2\frac{\partial\acute{v}}{\partial\acute{x}}\acute{\tau}_{yx}-2\frac{\partial\acute{v}}{\partial\acute{y}}\acute{\tau}_{yy}\right)=2\mu\frac{\partial\acute{u}}{\partial\acute{y}} \quad (11)$$

$$f\acute{\tau}_{zz}+k\left(\acute{u}\frac{\partial\acute{\tau}_{zz}}{\partial\acute{x}}+\acute{v}\frac{\partial\acute{\tau}_{zz}}{\partial\acute{y}}\right)=0$$

(12)

$$f\acute{\tau}_{xy}+k\left(\acute{u}\frac{\partial\acute{\tau}_{xy}}{\partial\acute{x}}+\acute{v}\frac{\partial\acute{\tau}_{xy}}{\partial\acute{y}}-\frac{\partial\acute{v}}{\partial\acute{x}}\acute{\tau}_{xx}-\frac{\partial\acute{v}}{\partial\acute{y}}\acute{\tau}_{xy}-\frac{\partial\acute{u}}{\partial\acute{x}}\acute{\tau}_{xy}-\frac{\partial\acute{u}}{\partial\acute{y}}\acute{\tau}_{yy}\right)=\mu\left(\frac{\partial\acute{u}}{\partial\acute{y}}+\frac{\partial\acute{u}}{\partial\acute{x}}\right)(13)$$

$$f=1+\frac{\varepsilon k}{\mu}\left(\acute{\tau}_{xx}+\acute{\tau}_{yy}+\acute{\tau}_{zz}\right)$$

(13)

In the equations above, scaling transformations are:

$$W_e=\frac{kc}{a},u=\frac{\acute{u}}{c},v=\frac{\acute{v}}{c\delta},x=\frac{\acute{x}}{\lambda},y=\frac{\acute{y}}{a},h=\frac{\acute{H}}{a},\delta=\frac{a}{\lambda},p=\frac{\acute{p}a^2}{\mu c\lambda},\theta=\frac{\acute{T}-\acute{T}_0}{\acute{T}_1-\acute{T}_0}\quad n=\frac{\acute{n}}{n_0},$$

$$t=\frac{c\acute{t}}{\lambda},Pr=\frac{\mu c_p}{K},Ec=\frac{c^2}{c_pT_0},\phi=\frac{b}{a},\tau_{ij}=\frac{a\tau_{ij}}{c\mu},R_d=\frac{-16\sigma\acute{T}^3}{3\kappa\mu c_f},Br=E_cPr,$$

$$E_c=\frac{c^2}{c_f\left(T_1-T_0\right)},\Re=\frac{\rho ca}{\mu}.$$

(15)

The conditions in (5) can be written as

$$h=1+\phi\sin(2\pi x)$$

(16)

We present transformations between fixed and wave frames.

$$\acute{x}=\acute{X}-c\acute{t},\acute{y}=\acute{Y},\acute{u}(\acute{x},\acute{y})=\acute{U}-c.\acute{v}(\acute{x},\acute{y})=\acute{v} \quad (17)$$

The appropriate non-dimensional boundary conditions corresponding to Saffman are:

$$\frac{\partial u}{\partial y}=0,v=0,at\ y=0$$

(18)

$$u=-1-\frac{\sqrt{Da}}{\alpha}\frac{\partial u}{\partial y},v=\frac{-dh}{dx},at\ y=h$$

(19)

$$\frac{\partial\theta}{\partial y}=0\, at\, y=0,\theta=1\, at\, y=h$$
(20)

With the help of equation (18) and under the condition of long wavelength and low Reynolds number $\delta\ll 1\wedge\Re\approx 0$, equations (6)-(14) takes the following form.

From momentum equation

$$\frac{\partial p}{\partial x}=\frac{\partial\tau_{xy}}{\partial x}$$
(21)

$$\frac{\partial p}{\partial y}=0$$
(22)

From fluid equation

$$f\tau_{xx}=2W_e\frac{\partial u}{\partial y}\tau_{xy}$$
(23)

$$f\tau_{yy}=0=f\tau_{zz},$$
(24)

$$f\tau_{xy}=W_e\frac{\partial u}{\partial y}\tau_{yy}+\frac{\partial u}{\partial y},$$
(25)

From energy equation

$$(1+PrRd)\frac{\partial^2\theta}{\partial y^2}=-Br\,\tau_{xy}\frac{\partial u}{\partial y},$$
(26)

Volume flow rate

The dimensional volume flow rate in laboratory frame is inscribed as

$$Q=\int_0^{\acute{h}}\acute{U}(\acute{X},\acute{Y},\acute{t})\,d\acute{Y}$$
(27)

where $\acute{h}=\acute{h}(\acute{X},\acute{t})$, in wave frame the above equation reduces

$$q=\int_0^{\acute{h}}u(\acute{x},\acute{y})\,d\acute{y}$$
(28)

in which

$\acute{h} = \acute{h}(\acute{x})$

From eq, $(26),(27) \wedge (28)$ one has

$Q = q + c\,\acute{h}(x)$
(29)

The time averaged over fixed frame $\acute{X}$ is

$\acute{Q} = \frac{1}{T}\int_0^T Q\,dt$
(30)

which after using Eq. (26) and performing integration leads to

$\theta = F + 1,$
(31)

where

$\theta = \frac{\acute{Q}}{ac}, F = \frac{q}{ac},$
(32)

$F = \int_0^h u dy$
(33)

Equation (24) tells that $\tau_{yy} = \tau_{zz} = 0$ and the stress tensors trace changes to τ_{xx}. Integration of Eq. (21) with $\tau_{xy} = 0\, at\ y = 0$ as the boundary condition (The line of symmetry yields) gives.

$\tau_{xy} = y\frac{dp}{dx}$
(34)

With help of equation (24) and (25), we can write

$\tau_{xx} = 2W_e\tau_{xy}^3$
(35)

From equations $(14),(24) \wedge (35)$ we get

$\frac{\partial u}{\partial y} = \tau_{xy} + 2\epsilon W_e^2\tau_{xy}^3$
(36)

Analytical Solution

Substituting Eq. (34) into Eq. (36) and then using the boundary conditions Eqs. (18) and (19), we get

$$u=-1-\frac{p\left(y^2-h^2\right)}{2}+\frac{2\epsilon W_e\left(y^4-h^4\right)}{4}-\frac{\sqrt{Da}}{\alpha}\left[ph+2\epsilon W_e p^3 h^3\right]$$
(37)

Making use of Eq. (37) into Eq. (33), we attain at

$$F=-h-\frac{h^2 p}{3}-\frac{\sqrt{Da}\,h^2 p}{\alpha}-\frac{2}{5}h^5 p^3 \epsilon W_e-\frac{2\sqrt{Da}\,h^4 p^3 \epsilon W_e}{\alpha}$$
(38)

Due to nonlinearity, it is difficult to arrive at the analytical solution to equation(38). As a result, the solution is obtained using the standard perturbation approach. We expand $p=\frac{dp}{dx}$ in terms of the parameter ($|W_e|$) in order to use the perturbation approach as follows:

$$p=p_0+W_e p_1$$
(39)

The solution of equation (39) is given by:

$$\frac{\partial p}{\partial x}=\left(\frac{6h^2 W_e}{5\left(3\sqrt{Da}+h\alpha\right)}\left(\frac{-135\sqrt{Da}\left(F+h\right)^3\alpha^3\epsilon}{h^6\left(3\sqrt{Da}+h\alpha\right)^3}-\frac{27\left(F+h\right)^3\alpha^4\epsilon}{h^5\left(3\sqrt{Da}+h\alpha\right)^3}\right)-\frac{3\left(F+h\right)\alpha}{h^2\left(3\sqrt{Da}+h\alpha\right)}\right)$$
(40)

On solving equation (26), with boundary condition equation (20), the solution of temperature is obtained as:

$$\theta=1+\frac{5\,Br\,p^2(h^4-y^4)+4\,Br\,p^4 W(h^6-y^6)\epsilon}{60\left(1+prRd\right)}$$
(41)

The pressure difference across the one wavelength is calculated from the previous equation

$$\Delta p=\int_0^1 \frac{\partial p}{\partial x}dx.$$

$$F_{\lambda}=\int_0^1 h\left(\frac{-\partial p}{\partial x}¿\right)dx.¿$$

Results and Discussions

In this section, the exact solutions that were calculated in the prior sector are now visually exhibited, allowing us to scrutinize the belongings of several (dimensionless) significant constraints on the flow profile, with W_e (Weissenberg number), ϵ(PTT parameter),Da (Darcy number) a (slip parameter), Rd(Thermal radiation parameter) Pr (Prandtl number) (i.e., temperature profile, velocity profile, pressure gradient, pressure rise). Since these graphical plots express the validity of mathematical solutions, the graphical parades permit a more exhaustive study of the existing effort. The graphical displays for the velocity and temperature profiles evidently show that the boundary conditions we used in our situation were in force. The associated equations and relevant boundary conditions are fully gratified by the calculated mathematical solutions. It is renowned that the axial velocity profiles show a parabolic character, which is a typical outcome for slip flow, where velocity is zero at the walls and greatest in the channel's center.

Flow characteristics

Figs. 2(a)-(c) show the effects of the physical factors on the material characteristics of the regulating fluid flow. Figure 2(a) demonstrations the conduct of the velocity profile with variable Darcy numbers (Da) there is a progressive decrease in the axial flow velocity with growingDa. The larger porosity parameter is associated with smaller permeability. Therefore, a smaller gap is available for fluid to flow, foremost to a reduction in velocity. Thus, a porous medium behaves like a resistive force that hinders fluid velocity. Outcome of α on $u$with$x$ is elucidates the Fig.2 (b). It has been exposed that when slip parameterα increases, the velocity profile rises. The impact of W_e is depicted in Fig. 2(c). From the figure, it is clear that Weissenberg number W_e drops the velocity of the liquid.

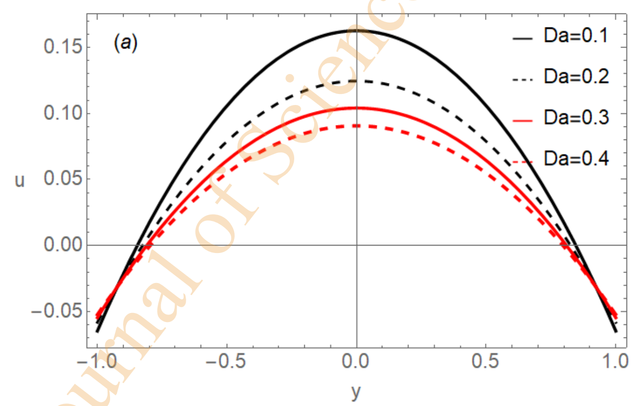

Fig.1. (a) Velocity distribution for diverse Da through $\Theta=0.95, \phi=0.6, \varepsilon=0.1, x=0.25$

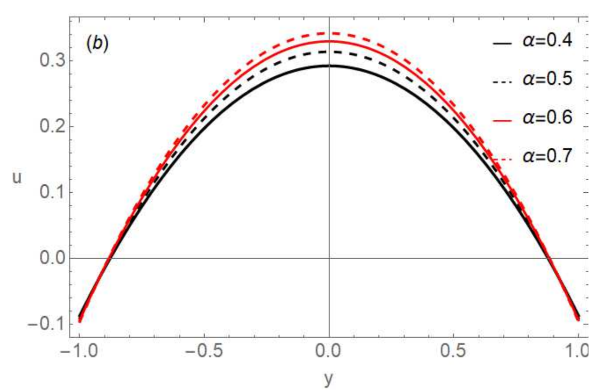

Fig.1. (b) Velocity distribution for diverse α through $\Theta=0.95, \phi=0.6, \varepsilon=0.1, x=0.25$

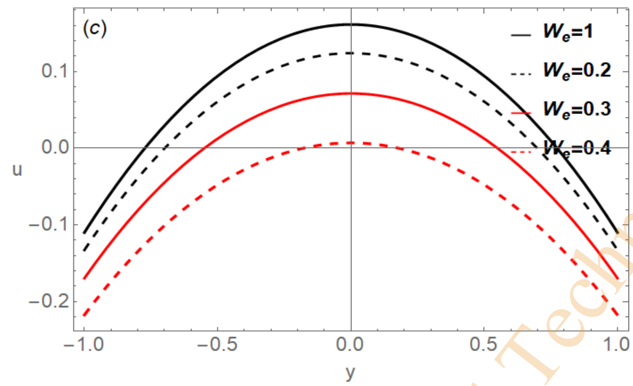

Fig.1. (c) Velocity distribution for diverse W_e through $\Theta=0.95, \phi=0.6, \varepsilon=0.1, x=0.25$.

Heat characteristics

In this sub part, the impacts of several influential parameter through the temperature field are discussed since it has comprehensive series of applications in manufacturing and mediational procedure. Hence the graphs of the temperature field for diverse values of W_e, Brinkmann number Br, Darcy number Da

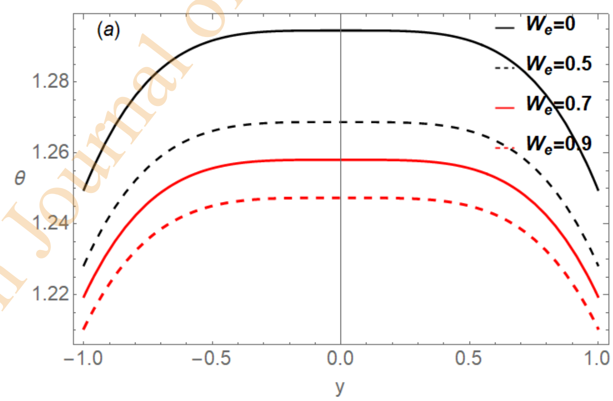

Fig.2. (a) Temperature distribution for diverse W_e through $\Theta=0.95, \phi=0.6, \varepsilon=0.1, x=0.25$

Prandtl number Pr, and thermal radiation Rd are displayed in Figs. 2(a)-(e) respectively. The impact of W_e is depicted in Fig. 2(a). From the figure, it is noted that the Weissenberg number W_e lowers the temperature of the liquid. The impact of Br through the fluid temperature is portrayed in Fig. 2(b). The figure articulates that the temperature of the liquid rises along with the Brinkmann number Br. Figs. (c)- (e) shows the temperature distribution for diverse values of Darcy number Da, PrandtlPr, and thermal radiation Rd it is depicted that with the increase in $Da, Pr, \wedge Rd$, the temperature profile declines.

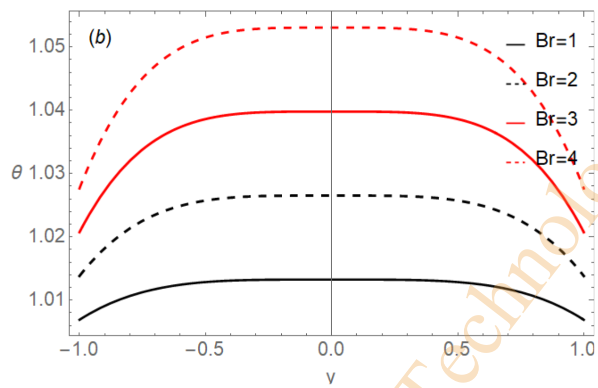

Fig.2. (b) Temperature distribution for diverse Br through $\Theta=0.95, \phi=0.6, \varepsilon=0.1, x=0.25$

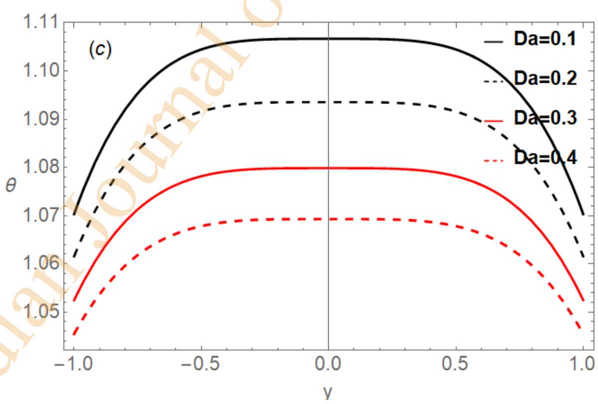

Fig.2. (c) Temperature distribution for diverse Da through $\Theta=0.95, \phi=0.6, \varepsilon=0.1, x=0.25$

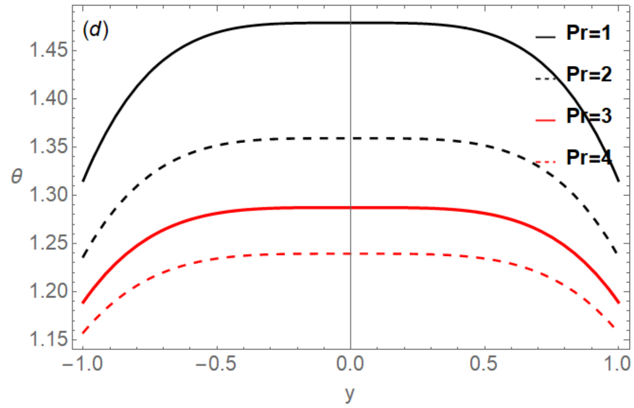

Fig.2. (d) Temperature distribution for diverse Pr through $\Theta=0.95, \phi=0.6, \varepsilon=0.1, x=0.25$

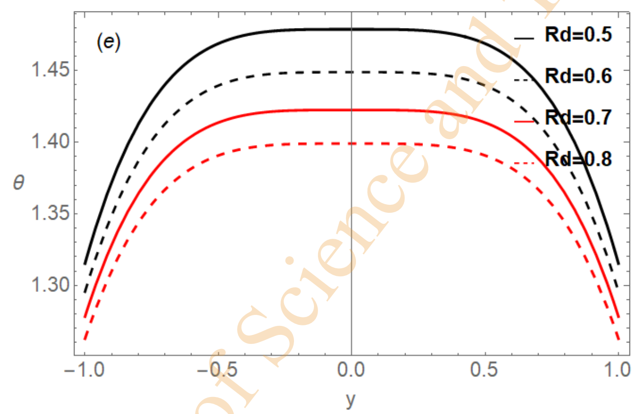

Fig.2. (e) Temperature distribution for diverse Rd through $\Theta=0.95, \phi=0.6, \varepsilon=0.1, x=0.25$

Pressure gradient

The axial pressure gradient profiles, or the pressure gradient vs the axial coordinate along the channel's center line in one period with fixed time and flow rate, are shown in Figs. 3(a)–3(c). Due to the nature of the peristaltic flow, it is evident that the pressure gradient profiles are uniform and display periodicity; specifically, they are minimal at fully relaxed wall sites and exhibit highest values at fully contracted wall sites. Additionally, we see in Figs. 3(a)–(c) that a negative pressure gradient always occurs in the channel due to the contraction and relaxation of the channel walls. It is observed that for $x \in [0, 0.5]$ and $[1, 1.4]$, the pressure gradient is minor, while the pressure gradient is large in the interval $[0.6, 0.9]$. Moreover, it is depicted that the pressure gradient escalations with upsurge in $W_e \wedge \alpha$ in the centre of the channel. Through Fig.3(c), we see that for a given Θ, the pressure falls with swelling Da.

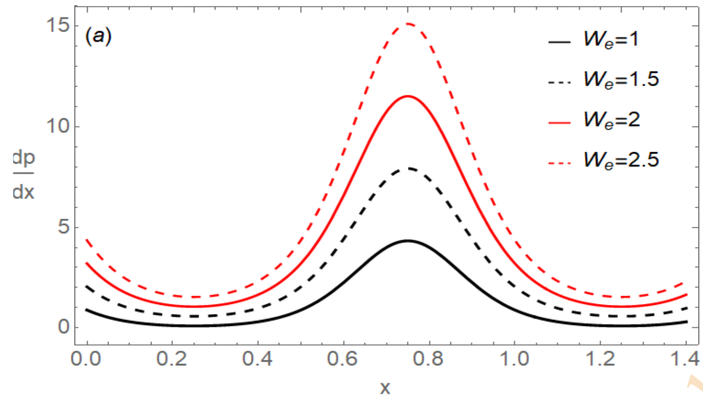

Fig.3. (a) Pressure gradient for diverse W_e through $\Theta=0.95, \phi=0.6, \varepsilon=0.1$

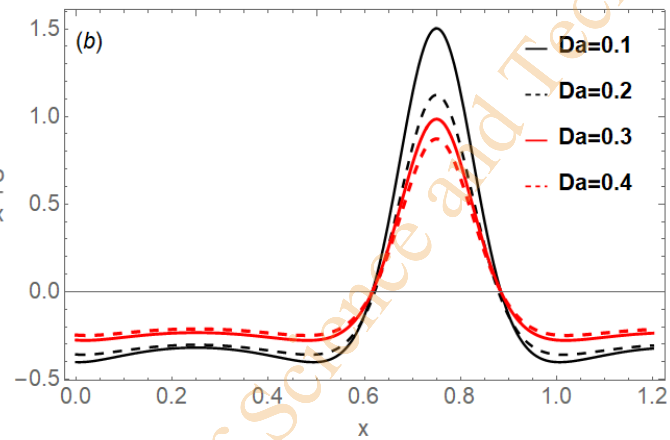

Fig.3. (b) Pressure gradient for diverse Da through $\Theta=0.95, \phi=0.6, \varepsilon=0.1$

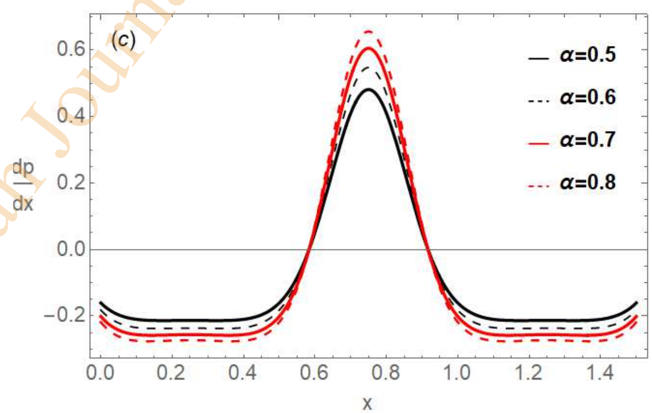

Fig.3. (c) Pressure gradient for diverse α through $\Theta=0.95, \phi=0.6, \varepsilon=0.1$

Pumping Characteristics

Well-known fact of peristaltic transport is connected with the perception of mechanical pumping. Therefore, it is justified ted to explore the performance pumping of in the view of existing study. This pumping allows for the controlled transfer of a volume of liquid from one area to another without any disturbance. Figs.4 (a)-3(c) shows the change in pressure rise Δp with respect to flow rate$Q$.A linear relation between the flow rate and pressure is observed and there are three pumping regions: (i) pumping region$(\Delta p>0)$. (ii) free pumping region $(\Delta p=0)$ and (iii) augmented pumping region$(\Delta p<0)$. The effect of Weissenberg numberW_e on increase in pressure is shown in Fig. 4(a) and it is evident that the pressure diminishes with an increasing in W_e in the pumping region where as the opposite response is computed in the augmented pumping region. From Fig.4 (b), it is seen that the rise in pressure is an increasing function of amplitude in pumping region where as it is decreasing function in augmented pumping region. The impact of Darcy number on pressure rise is illustrated in 4(c) and exerts a similar effect with Weissenberg numberW_e.

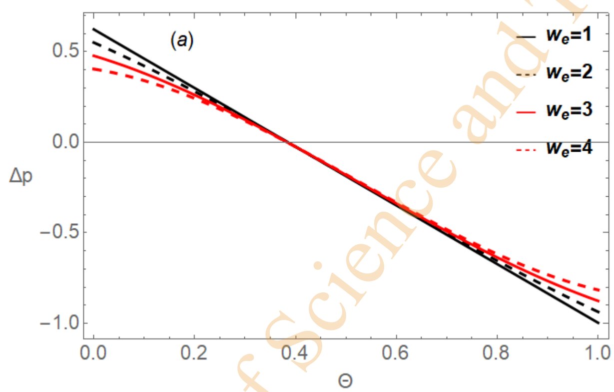

Fig.4. (a) Pressure rise for diverse W_e through $x=0.25, \phi=0.6, \varepsilon=0.1$

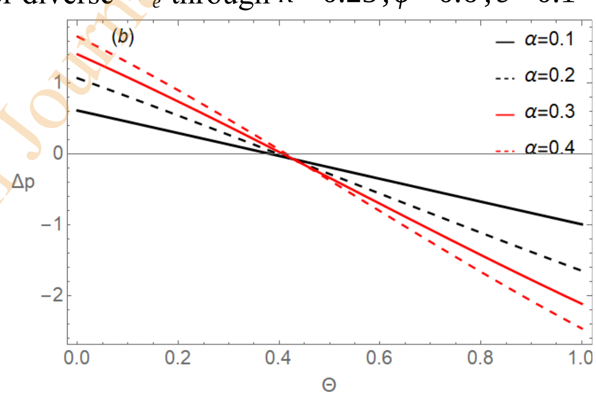

Fig.4. (b) Pressure rise for diverse α through $x=0.25, \phi=0.6, \varepsilon=0.1,$

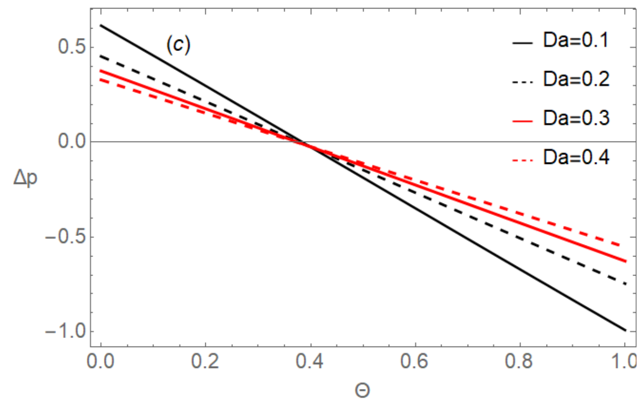

Fig.4. (c) Pressure rise for diverse Da through $x=0.25, \phi=0.6, \varepsilon=0.1$

4. Conclusion

In this study, a mathematical study has been conducted on peristaltic flow induced by heat and thermal radiation in viscous propulsion through a permeable channel. The main focus of this study is to highlight the effects of thermal radiation, permeable walls, and Phan-Thien-Tanner (PTT) model parameters on velocity, temperature, pressure gradient, and pressure rise phenomena. Understanding these phenomena is crucial for both physiological and industrial applications of peristaltic transport. The major findings of this work are as follows:

1. Velocity is decreasing function for $W_e \wedge$¿Da whereas it is an increasing function of slip parameter.
2. The temperature enhances with increasing values of $W_e \wedge Br$.
3. The pressure gradient increases with increasing Weissenberg number W_e and slip parameter α.
4. Pressure gradient reduces with increasing permeability (higher Darcy number).
5. Pressure rise reduces with increasing permeability (higher Darcy number) and Weissenberg number$(W$¿¿$e)$¿, in the pumping region whereas the reverse trend is observed in the augmented pumping region.

5. References

1. Latham, T.W, Fluid motions in peristaltic pump, M.S Thesis, *M.I.T. Massachusetts Institute of Technology*, Cambridge. 1966:7: 1-74.
2. Shapiro A, Jaffrin M, and Weinberg H Peristaltic pumping with long wavelength at low Reynolds number. *Journal of Fluid Mechanics.* 1969:35**:** 799-825.
3. Hayat T, Farooq S, Ahmed B and Alsaedi A Characteristics of Convective heat transfer in the MHD peristalsis of Carreau fluid with Joule heating. *AIP Advances*. 2016:6**:** 045302.
4. Akbar N, Nadeem S, and Khan Z Numerical simulation of peristaltic flow of a Carreau nanofluid in a asymmetric channel. *Alexandria Engineering. Journal*. 2014:53**:** 191-197.

5. Rathod, V. P. and Mahadev, M. Peristaltic flow of Jeffrey fluid with slip effect in an inclined channel. *Journal of Chemical Biological Physics.*2012: 2:1987–1997.
6. Rathod, V. P. and Channakote, M. M.A study of ureteral peristalsis in a cylindrical tube through a porous medium. *Advances in Applied Science and Research.* 2011:3:134–140.
7. Srinivas, A.N.S, Hemadri Reddy, R. Peristaltic transport of a casson fluid in a channel with permeable walls. *International Journal of Pure and Applied Mathematics*. 2014:90:1: 11-24.
8. Vajravelu, K, Sreenadh, S, Hemadri Reddy, R, Murugesan, K. Peristaltic Transport of a casson fluid in contact with Newtonian fluid in a circular tube with Permeable wall. *International Journal of Fluid Mechanics Research*. 2009:36:3:244-254.
9. Akhtar, S, Luthais McCash, B, Nadeem, S, Saleem, S and Issakhov, A, Mechanics of non-Newtonian blood flow in an artery having multiple stenosis and electroosmotic effects. *Science Programme*, 2009:104:1–15
10. Prakash Goswami, Pranab Kumar Mondal, Anubhab Datta and Suman Chakraborty. Entropy generation minimization in an electroosmotic flow of non-Newtonian fluid: effect of conjugate heat transfer", *ASME Journal of Heat Transfer*, 2016:138:5:051704
11. Misra and Ramachandra Rao, A. Peristaltic transport of non-Newtonian fluid in asymmetric channel. *Journal of Applied Mathematical Physics*. 2003:54:532-50.
12. Hakeem Abd EI, Nabby Abd EI.Creeping Flow of Phan-Thien–Tanner fluids in a peristaltic tube with an infinite long wavelength", American Society of Mechanical Engineers, *Journal of Applied Mathematics*. 2009:76:064504.
13. Vajravelu, K, Sreenadh, S, Dhananjaya, S, Lakshminarayana, P. Peristaltic flow and heat transfer of a conducting Phan-Thien-Tanner fluid in an asymmetric channel- application to chyme movement in small intestine. Indian Institute of Technology, *Journal of Applied Mechanics and Engineering*. 2016:21:3:713-736.
14. Hayat, T, Noreen, S, Ali, N, Abbasbanday, S. Peristaltic motion of Phan-Thien-Tanner fluid in a planner channel. *Numerical. Method. Partial Differential. Equations*, 2010:28**:** 738-748.
15. Abd El Hakeem Abd El Naby. Creeping Flow of Phan-Thien–TannerFluids in a Peristaltic Tube Withan Infinite Long Wavelength. *Journal of Applied Mechanics*. 2009:**76**:064504-1.
16. Siddiqui, A.M. Azim, Q. A. Ashraf, A. and Ghori, Q. K. Exact Solution for Peristaltic Flow of PTT Fluid in an Inclined Planar Channel and Axisymmetric Tube. *International Journal of Nonlinear Sciences and Numerical Simulation*. 2009:10:75-92.
17. Hayat, T., Noorin, S. Ali, N. Abbasbandy. Peri-staltic motion of Pan-Thien-Tanner fluid in a planar channel. *Numerical methods for Partial Differen-tial Equations*. 2012: 28:737-748.
18. Mahadev, M. and Axita Mohanta. Thermal radiation effect on Pan-Thien-Tanner liquid model obeying peristaltic activity with cilia waves". World Scientific News. 2023:183: 2010-2026.
19. Vajravelu, K., Sreenadh, S, Laxminarayana, P. Suchari-tha, G. and. Rashidi, M.M. The peristaltic flow of Phan-Thien-Tanner fluid in an asymmetric channel with porous medium, Journal of Applied Fluid Mechanics. 2016:9:1615-1625.
20. Channakote, M. Shekar. M. Dilipkumar, V.K. electro-osmotic effect on peristaltic flow of phan–thien–tanner fluid in a planar channel. The Anziam journal. Published online 2024:1-21.

21. Vajravelu, K. Sreenadh, S. Lakshminarayana, P. Sucharitha, G. and Rashidi, M.M. Peristaltic flow of Phan-Thien-Tanner fluid in an asymmetric channel with porous medium. *Journal of Applied Fluid Mechanics*.2015:9**:**1615-1625.
22. Radhakrishnamacharya, G and Radhakrishnamurty, V. Peristaltic flow and heat transfer in a vertical porous medium, *Applied Mathematics and Computer*. 2007:153:763-777.
23. Channakote, M.M and Kalse, M.V. Heat Transfer in Peristaltic Motion of Rabinowitsch Fluid in a Channel with Permeable Wall. *Applied Mathematics.* 2021:16**:**1, 1-19.
24. Mekheimer, Kh.S. and Abd Elmaboud, Y. Peristaltic flow through a porous medium in an annulus: Application of an endoscope. *Applied Mathematics & Information Sciences*.2008:2:103-121.
25. Srinivas, S and Gayathri, R. Peristaltic transport of a Newtonian fluid in a vertical asymmetric channel with heat transfer and porous medium. *Applied Mathematics Computer***.** 2009:215: 1855-196.
26. Anas A.M. Arafa, Sameh E. Ahmed, Allan, M.M. Peristaltic flow of non-homogeneous nanofluids through variable porosity and heat generating porous media with viscous dissipation: Entropy analyses *Case Studies in Thermal Engineering*.2022:32: 101882.
27. Rafiq, M., Shaheen, A., Trabelsi, Y. et al. Impact of activation energy and variable properties on peristaltic flow through porous wall channel. *Science Report*. 2023:13: 3219.
28. Eldabe, N. T. M. Shaker, M. O. and Maha, S. A. Peristaltic Flow of MHD Jeffrey fluid through porous medium in a vertical channel with heat and mass transfer with radiation. *Journal of Nanofluid.*2018:7: .595–602.
29. Sunitha, G, and Asha, S.K. Influence of thermal radiation on peristaltic blood flow of a Jeffrey fluid with double diffusion in the presence of gold nanoparticles. *Inf. in Med. Unl*. 2019:17**:**1-13.
30. Kothandapani, M. and Prakash, J. Effects of thermal radiation parameter and magnetic field on the peristaltic motion of Williamson Nano fluids in a tapered asymmetric channel", Indian Institute of Technology, *Journal of Heat and Mass Transfer*, 2015:81:234-245.
31. Rafiq, M.Y, Abbas, Z. Impacts of viscous dissipation and thermal radiation on Rabinowitsch fluid model obeying peristaltic mechanism with wall properties. Arab., *Journal of Science and English*. 2021:12**.**05870-7.
32. Hayat, T. Saima Rani, Alsaedi, A. Rafiq, M. Radiative peristaltic flow of magneto nanofluid in a porous channel with thermal radiation", *Results in Physics*. 2021:7:3396-3407.
33. Kotnurkar, A.S. and Talawar, V.T. Impact of electro osmosis and joule heating effects on peristaltic transport with thermal radiation of hyperbolic tangent fluid through a porous media in an endoscope. *Partial Differential Equations in Applied Mathematics*.2022: 10.1016/j.padiff.2022.100340.
34. Channakote, M.M. and Siddabasappa, C. Heat and mass transfer analysis on peristaltic transport of PTT fluid with wall properties, *Latin American Applied Research*.54:2024:1-9.
35. Channakote, M. M. and Kalse, V. D. Combined convective and viscous dissipation effects on peristaltic flow of Ellis fluid in non uniform tube. *Journal of Naval Architecture and Marine Engineering*. 2022:19:1–12.

36. Adil Wahid, B, Akbar, N.S, Mir, N.A. Heat transfer analysis of peristaltic flow of a Phan-Thien-Tanner fluid model due to metachronal wave of cilia. *Biomechanics and modelling in mechanobiology*. 2020:19:5:1925-1933
37. Hussain, S, Ali, N. and Ullah, K. Peristaltic flow of Phan-Thien-Tanner fluid: effects of peripheral layer and electroosmotic force. *Rheological. Acta*. 1977:58**:**603-618.
38. Naveed, Imran, M, Sohail, J, M, Iskander, Tlili Simultaneous effects of heterogeneous-homogeneous reactions in peristaltic flow comprising thermal radiation: Rabinowitsch fluid model. *Jmr & t,* 2020:9:3:520-3529.
39. Noreen, S. Pressure driven flow of PTT fluid in a channel with heat transfer and inclined magnetic field. *International. Journal of Applied Computer and Mathematics*. 2017:3:497–1509.
40. Asha, S.K. Sunitha, G. Thermal radiation and Hall effects on peristaltic blood flow with double diffusion in the presence of nanoparticles, *Case Studies in Thermal* Engineering. 2020:17: 100560.